**List of Tables**

Table 1

| Catalyst | Preparation method | Reaction conditions | HCHO conversion/removal | Reference |
|---|---|---|---|---|
| 1 wt% $Pd/TiO_2$ | Deposition precipitation-reduction | 500 mg catalyst, 10 ppm HCHO, air, 50% [3]RH, 120,000 mL/g·h [5]GHSV | [2]100% at 25°C | (*33*) |
| 1 wt% $Au/CeO_2$ | Deposition precipitation (using urea) | 250 mg catalysts,80 ppm HCHO, 21%$O_2/N_2$, 50% [3]RH, 34,000/h [5]GHSV | [1]100% at 25°C | (*58*) |
| 1 wt% $Au/CeO_2$ | Deposition precipitation (using NaOH) | 250 mg catalyst, 80 ppm HCHO, 21%$O_2/N_2$, 50% [3]RH, 34,000/h [5]GHSV | [1]100% at 70°C | (*58*) |
| 2 wt% Na−1 wt% $Pd/TiO_2$ | Impregnation-reduction | 65 mg catalyst, 140 ppm HCHO, 20% $O_2$, 25% [3]RH, 95,000/h [5]GHSV | [1]100% at 25°C | (*59*) |
| 0.8 wt% Pt/AlOOH | Impregnation-reduction | 100 mg catalyst, 138 ppm HCHO, air, 25% [3]RH | [2]96.82% [4](25°C,1h) | (*60*) |
| 0.8 wt% $Pt/TiO_2$ | Impregnation-reduction | 100 mg catalyst, 138 ppm HCHO, air, 25% [3]RH | [2]96.82% [4](25°C,1h) | (*60*) |
| $Ag/CeO_2$ (nanosphere) | Hydrothermal synthesis | 50 mg catalyst, 810 ppm HCHO, 20% $O_2$, and balance $N_2$, 84,000/h [5]GHSV | [1]100% at 110°C | (*47*) |
| Ag/3D-$Co_3O_4$ | Deposition-precipitation | 200 mg catalyst, 100 ppm HCHO, 20% $O_2$, 30,000/h [5]GHSV | [1]100% at 100°C | (*46*) |
| 1.7wt% K- Ag/3D-$Co_3O_4$ | Deposition-precipitation | 200 mg catalyst, 100 ppm HCHO, 20% $O_2$, 30,000/h [5]GHSV | [1]100% at 70°C<br>[1]55% at 27°C | (*46*) |
| 8.9 wt% Ag/3D- $MnO_2$ | Deposition-precipitation | 200 mg catalyst, 500 ppm HCHO, 20% $O_2$, 60,000/h [5]GHSV | [1]100% at 110°C | (*43*) |
| $Ag/MnO_2$ | Redox-reaction | 200 mg catalyst, 230 ppm HCHO, air, static reactor | [1]76% [4](25°C,1h) | (*61*) |
| $Ag/Fe_{0.1}$- $MnO_2$ | Redox-reaction | 200 mg catalyst, 230 ppm HCHO, air, static reactor | [1]100% [4](25°C, 1h) | (*61*) |
| $Ag/MnO_2$ | Redox-reaction | 200 mg catalyst, 400 ppm HCHO, 21% $O_2$, 30,000 mL/g·h [5]GHSV, dynamic system | [1]100% at 120°C | (*61*) |
| $Ag/Fe_{0.1}$- $MnO_2$ | Redox-reaction | 200 mg catalyst, 400 ppm HCHO, 21% $O_2$, 30,000 mL/g·h [5]GHSV, dynamic system | [1]100% at 90°C | (*61*) |
| 3DOM-$Au/CeO_2$ | Nanocasting: Polystyrene colloidal crystal hard templates | 200 mg catalyst, 0.06% HCHO, purified air, 66,000 mL/ g·h [5]GHSV | [1]100% at 75°C | (*44*) |
| 0.85 wt% $Au/ZrO_2$-silicate | Deposition | 200 mg catalyst, 90 mg/$m^3$ HCHO, purified air, 52,000 ml/g·h [5]GHSV | [1]100% at 157°C | (*62*) |
| 3 wt% $Au/CeO_2$ | Deposition-precipitation | 50 mg catalyst, 500 ppm HCHO, 20% $O_2$, 35,400/h [5]GHSV | [1]92.3% at 37°C and [1]100% at 50°C | (*37*) |
| 7.10 wt% $Au/Fe_2O_3$ | Co-precipitation | 200 mg catalyst, 6.25mg/$m^3$ HCHO, compressed air, 54,000 ml/g·h [5]GHSV | [1]100% at 80°C | (*63*) |
| 1.8 wt % $Au/CeO_2$ | Deposition-precipitation | 150 mg catalyst, 109.3 ppm HCHO, air, static reactor | [2]90% (25°C, 1h) | (*64*) |
| 2 wt Pt/urchin-like $MnO_2$ | RT redox reaction | 100 mg catalyst, 460 ppm, purified air 20,000 mL/ g·h [5]GHSV | [1]100% at 80°C | (*41*) |

| | | | | |
|---|---|---|---|---|
| 2 wt% Pt/cocoon-like MnO2 | Redox reaction under acidic condition | 100 mg catalyst, 460 ppm HCHO, purified air 20,000 mL/ g·h [5]GHSV | [1]100% at 90°C | (*41*) |
| Pt/OMS-2 | Redox reaction plus impregnation | 200 mg catalyst, 500 ppm HCHO, 10% $O_2$, 30,000 ml/ g·h [5]GHSV | [1]100% at 120°C | (*45*) |
| 0.2 wt% Pt/0.5 wt% $MnO_2/TiO_2$ (Nanotubes) | Electrochemical anodization plus impregnation | 200 mg catalyst, 50 ppm HCHO, 20% $O_2$, 35% [3]RH, 30,000 ml/g·h [5]GHSV | [2]95% at 30°C | (*65*) |
| 0.1 wt% $Pt/TiO_2$ | Impregnation-reduction | 500 mg catalyst, 10 ppm HCHO, air, 50% [3]RH, 80,000/h [5]GHSV | [2]99.1% at 25°C | (*24*) |
| 2 wt% Na-1 wt% $Pt/MnO_2$ (birnessite) | Deposition-precipitation | 100 mg catalyst, 200 ppm HCHO, purified air, 30,000 mL/g·h [5]GHSV | [1]100% at 50°C | (*66*) |
| NaOH modified - 1 wt% $Pt/TiO_2$ | Impregnation-reduction | 300 mg catalyst, 253 ppm HCHO, air, static reactor | [2]94.07% [4](25°C, 1h) | (*27*) |
| 1 wt% $Pt/TiO_2$ | Impregnation | 100 ppm HCHO, 20 vol% $O_2$, 50,000/h [5]GHSV | [1]100% at 20°C | (*22*) |
| 1 wt% $Rh/TiO_2$ | Impregnation | 100 ppm HCHO, 20 vol% $O_2$, 50,000/h [5]GHSV | [1]100% at 80°C | (*22*) |
| 1 wt% $Pd/TiO_2$ | Impregnation | 100 ppm HCHO, 20 vol% $O_2$, 50,000/h [5]GHSV | [1]100% at 120°C | (*22*) |
| 3D 3wt% Au/ $CeO_2$-$Co_3O_4$ (2.5:1, Ce/Co) | Nanocasting: 3D-PS hard template | 200 mg catalyst, 8 ppm HCHO, purified air, 15,000 mL/g·h [5]GHSV | [1]100% at 36°C | (*50*) |
| 2D 1wt% Au/ $Co_3O_4$-$CeO_2$ (7:3 Co:Ce) | Nonocasting: SBA-15 hard template | 100 mg catalyst, 200 ppm HCHO, 22% $O_2$, 55,000/h [5]GHSV | [1]50% at 25°C | (*51*) |
| 3 wt% Pt/$MnO_x$-$CeO_2$ (M.R = 0.5) | Impregnation | 200mg catalyst, 30-580 ppm HCHO, 20% $O_2$, 30,000 mL/g·h [5]GHSV | [1]100% at 25°C | (*48*) |

[1] Conversion = $[CO_2]_{out}$ / $[HCHO]_{in}$

[2] Removal = ($[HCHO]_{in}$ - $[HCHO]_{out)}$ / $[HCHO]_{in}$

[3] RH - Relative humidity

[4] Indicates the reaction temperature and time taken to reach stated removal/conversion in a static reactor.

[5]GHSV- Gas hourly space velocity ($h^{-1}$ or ml/g.h)

Table 2

| Catalyst | Preparation method | Reaction conditions | HCHO conversion/removal | Reference |
|---|---|---|---|---|
| Birnessite | Hydrothermal synthesis using surfactant (SDS) | 100 mg catalyst, 460 ppm HCHO, purified air, 30,000 ml/g·h [5]GHSV | [1]100% at 100°C | (*54*) |
| Birnessite | Redox Reaction of $KMnO_4$ and Ammonium oxalate | 100 mg catalyst , 40 ppm HCHO, air, 80% [3]RH, 120,000 ml/g·h, | [1]90% at 96°C | (*74*) |
| Birnessite | Surface modification of birnesite with nitric acid and Tetraammonium hydroxide | 100 mg catalyst, 200 ppm HCHO, air, , 45% [3]RH, 120,000 ml/g·h [5]GHSV | [1]100% at 100°C | (*75*) |
| Todorokite | Na-Birnesite followed by $MgCl_2$ hydrothermal treatment | 200 mg catalyst, 400 ppm HCHO, 10.0% $O_2$, 18,000 ml/g·h [5]GHSV | [1]100% at 160°C | (*55*) |
| Pyrolusite | Redox hydrothermal synthesis | 200 mg catalyst, 400 ppm HCHO, 10.0% $O_2$, 18,000 ml/g·h [5]GHSV | [1]100% at 180°C | (*55*) |
| K-OMS-2 nanoparticle | Soft chemistry ($KMnO_4$ and benzyl alcohol) using surfactant (CTAB) at 25°C | 100 mg catalyst, 460 ppm HCHO, purified air, 20,000 ml/g·h [5]GHSV | [1]64% at 100°C. | (*56*) |
| K-OMS-2 nanorod | Soft chemistry ($KMnO_4$ and benzyl alcohol) using surfactant (CTAB) at 100°C | 100 mg catalyst, 460 ppm HCHO, purified air, 20,000 ml/g·h [5]GHSV | [1]10% at 100°C | (*56*) |
| K-OMS-2 nanorods | Sol-gel synthesis at 70°C | 100 mg catalyst, 460 ppm HCHO, 21% $O_2$, 30,000 ml/g·h [5]GHSV | [1]100% at 200°C | (*36*) |
| K-OMS-2 nanoparticles | Sol-gel synthesis at 15°C | 100 mg catalyst, 460 ppm HCHO, 21% $O_2$, 30,000 ml/g·h [5]GHSV | [1]54% at 200°C | (*36*) |
| OMS-2 | Redox reaction | 200 mg catalyst, 500 ppm HCHO, 10% $O_2$, 30,000 ml/g·h [5]GHSV | [1]100% at 120°C | (*45*) |
| 3D-$MnO_2$ mesoporous | Nanocasting: KIT-6 hard template | 200 mg catalyst, 400 ppm HCHO, 20% $O_2$, 30,000 ml/g·h [5]GHSV | [1]100% at 130°C | (*76*) |
| α-$MnO_2$ nanorods | Redox-hydrothermal synthesis | 200 mg catalyst, 400 ppm HCHO, 20% $O_2$, 30,000 ml/g·h [5]GHSV | [1]100% at 140°C | (*76*) |
| β-$MnO_2$ nanorods | Redox-hydrothermal synthesis | 200 mg catalyst, 400 ppm HCHO, 20% $O_2$, 30,000 ml/g·h [5]GHSV | [1]100% at 180°C | (*76*) |
| 8.86% $MnO_2$/cellulose (nanosheet birnessite) | $KMnO_4$ impregnation followed by oleic acid reduction | 60 mg catalyst, 100 ppm HCHO, 20% $O_2$, 50, 000/h [5]GHSV | [2]100% at 140°C | (*82*) |
| Birnessite nanospheres | $KMnO_4$-oleic acid hydrothermal reduction | 50 mg catalyst, 100 ppm HCHO, 20% $O_2$, 50,000/h [5]GHSV | [2]100% at 140°C | (*77*) |
| Cryptomelane nanorods | $KMnO_4$-oleic acid hydrothermal reduction | 50 mg catalyst, 100 ppm HCHO, 20% $O_2$, 50,000/h [5]GHSV | [2]95.1% at 140°C | (*77*) |
| Ramsdellite nanorods | $KMnO_4$ oleic acid hydrothermal reduction | 50 mg catalyst, 100 ppm HCHO, 20% $O_2$, 50,000/h [5]GHSV | [2]87.2% at 140°C | (*77*) |
| Monoclinic MnOOH | $KMnO_4$ oleic acid hydrothermal reduction | 50 mg catalyst, 100 ppm HCHO, 20% $O_2$, 50,000/h [5]GHSV | [2]90.1% at 140°C | (*77*) |

| | | | | |
|---|---|---|---|---|
| KxMnO$_2$ mesoporous hollow nanospheres | Low concentration KMnO$_4$-oleic acid reduction | 50 mg catalyst, 100 ppm HCHO, 20% O$_2$, 50,000/h [5]GHSV | [2]100% at 80°C | (*21*) |
| KxMnO$_2$ mesoporous honeycomb nanospheres | High concentration KMnO$_4$-oleic acid reduction | 70 mg catalyst, 100 ppm HCHO, 20% O$_2$, 50,000/h | [2]100% at 85°C | (*21*) |
| Birnessite | Facile redox-reaction | 50 mg catalyst, 200 ppm HCHO, synthetic air, static reactor | [2]100% [4](25°C,12h) | (*73*) |
| α-MnO$_2$ | Hydrothermal synthesis | 60 mg catalyst, 170 ppm HCHO, 20% O$_2$, 25% [3]RH, 100,000 mL/g·h [5]GHSV | [1]100% at 125°C | (*19*) |
| β-MnO$_2$ | Hydrothermal synthesis | 60 mg catalyst, 170 ppm HCHO, 20% O$_2$, 25% [3]RH, 100,000 mL/g·h [5]GHSV | [1]100% at 200°C | (*19*) |
| γ-MnO$_2$ | Hydrothermal synthesis | 60 mg catalyst, 170 ppm HCHO, 20% O$_2$, 25% [3]RH, 100,000 mL/g·h [5]GHSV | [1]100% at 150°C | (*19*) |
| δ-MnO$_2$ | Hydrothermal synthesis | 60 mg catalyst, 170 ppm HCHO, 20% O$_2$, 25% [3]RH, 100,000 mL/g·h [5]GHSV | [1]100% at 80°C | (*19*) |
| Spinel Co$_3$O$_4$ | Precipitation with KHCO$_3$ | 100 mg catalyst, 100 ppm HCHO, 21% O$_2$, 69,000/h [5]GHSV | [1]100% at 90°C | (*67*) |
| Spinel Co$_3$O$_4$ | Precipitation with NH$_4$HCO$_3$ and 2% K$_2$CO$_3$ treatment | 100 mg catalyst, 100 ppm HCHO, 21% O$_2$, 69,000/h [5]GHSV | [1]100% at 90°C | (*67*) |
| Spinel Co$_3$O$_4$ | Precipitation with KOH | 100 mg catalyst, 100 ppm HCHO, 21% O$_2$, 69,000/h | [1]100% at 120°C | (*67*) |
| Spinel Co$_3$O$_4$ | Precipitation with NH$_3$·H$_2$O | 100 mg catalyst, 100 ppm HCHO, 21% O$_2$, 69,000/h [5]GHSV | [1]100% at 130°C | (*67*) |
| 3D- Co$_3$O$_4$ | Nanocasting: KIT-6 hard template | 200 mg catalyst, 400 ppm HCHO, 20% O$_2$, 30,000 ml/g·h [5]GHSV | [1]100% at 130°C | (*70*) |
| 2D- Co$_3$O$_4$ | Nanocasting: SBA-15 hard template | 200 mg catalyst, 400 ppm HCHO, 20% O$_2$, 30,000 ml/g·h [5]GHSV | [1]100% at 150°C | (*70*) |
| Nano- Co$_3$O$_4$ | Precipitation with Na$_2$CO$_3$ | 200 mg catalyst, 400 ppm HCHO, 20% O$_2$, 30,000 ml/g·h [5]GHSV | [1]100% at 230°C | (*70*) |
| 3D- Co$_3$O$_4$ | Nanocasting: KIT-6 hard template | 200 mg catalyst, 100 ppm HCHO, 20% O$_2$ , 30,000/h [5]GHSV | [1]100% at 110°C | (*46*) |
| 3D-Cr$_2$O$_3$ | Nanocasting: KIT-6 hard template | 100 mg catalyst, 500 ppm HCHO, 30,000 ml/g·h [5]GHSV | [1]90% at 117°C | (*69*) |
| 2D- Co$_3$O$_4$ | Nanocasting: SBA-15 hard template | 100 mg catalyst, 200 ppm HCHO, 22% O$_2$, 55,000/h [5]GHSV | [1]20.3% at 25°C | (*51*) |
| Co$_3$O$_4$ nanofibers | spiral electrospinning synthesis, calcined at 500°C | 100 mg catalyst, 400 ppm HCHO, 20% O$_2$, 30,000 mL/g·h [5]GHSV | [1]100% at 98°C | (*78*) |
| 4% Eu doped-CeO$_2$ nanosheets | Anodic electrodeposition of Eu onto CeO$_2$ | 200 mg catalyst, 50 ppm HCHO, 25% O$_2$, 30,000mL/g·h [5]GHSV | [2]100% at 120°C | (*80*) |
| H-TiO$_2$ | Hydrothermal synthesis | 100 mg catalyst, 100 ppm HCHO, air, static reactor | [2]53% at [4](25°C,4h) | (*81*) |

[1] Conversion = $[CO_2]_{out}$ / $[HCHO]_{in}$

[2] Removal = ($[HCHO]_{in}$ - $[HCHO]_{out)}$ / $[HCHO]_{in}$

[3] RH - relative humidity

[4] Indicates the reaction temperature and time taken to reach such conversion in a static reactor.

[5]GHSV- Gas hourly space velocity ($h^{-1}$ or ml/g.h)

Table 3

| Catalyst | Preparation method | Reaction conditions | HCHO conversion/removal | Reference |
|---|---|---|---|---|
| $MnO_x$-$CeO_2$ | Co-precipitation | 200 mg catalyst, 580 ppm HCHO, 18% $O_2$, 21,000 mL/g·h [4]GHSV | [1]100% at 100°C | (*86*) |
| $MnO_x$-$CeO_2$ | Co-precipitation | 200 mg catalyst, 580 ppm HCHO, 20% $O_2$, 30,000 mL/g·h [4]GHSV | [1]90% at 90°C | (*48*) |
| $Mn_{0.5}Ce_{0.5}O_2$ | Co-precipitation | 300 mg catalyst, 33 ppm HCHO, 21% $O_2$, 10,000/h [4]GHSV | [2]100% at 270°C | (*93*) |
| $Mn_{0.5}Ce_{0.5}O_2$ | Co-precipitation | 300 mg catalyst, 61 ppm HCHO, 21% $O_2$/506 ppm HCHO $O_3$, 10,000/h [4]GHSV | [2]100% at 25°C | (*93*) |
| $MnO_x$-$CeO_2$ | Co-precipitation | 200mg catalyst, 580 ppm HCHO, 20% $O_2$, 30,000 mL/g·h [4]GHSV | [1]100% at 125°C | (*92*) |
| Ce-$MnO_2$ | Redox reaction of $KMnO_4$ and Ammonium oxalate with Cerium nitrate | 100 mg catalyst, 190 ppm HCHO, air, 90 L/g·h [4]GHSV | [1]100% at 100°C | (*94*) |
| 3D-$CeO_2$- $Co_3O_4$ | Nanocasting: 3D-PS hard template | 200 mg catalyst, 8 ppm HCHO, purified air, 15,000 mL/g·h [4]GHSV | [1]100% at 155°C | (*50*) |
| Co-Mn | Co-precipitation | 150 mg catalysts, 80 ppm HCHO, 21% $O_2$, 50% [3]RH, 60,000/h [4]GHSV | [1]100% at 75°C | (*95*) |
| 3D-Co-Mn | Nanocasting: KIT 6 Hard template | 250 mg catalyst, 80 ppm HCHO, 21% $O_2$, 50% [3]RH, 36,000/h [4]GHSV | [1]100% at 70°C | (*68*) |
| $MnO_x$-$Co_3O_4$-$CeO_2$ | Sol-gel synthesis | 50 mg catalyst, 200 ppm HCHO, 21% $O_2$, 36,000 ml/g·h [4]GHSV | [1]100% at 100°C | (*96*) |
| $MnO_x$-$SnO_2$ | Redox co-precipitation | 200 mg catalyst, 400 ppm HCHO, 10% $O_2$, 30,000 ml/g·h [4]GHSV | [1]100% at 180°C | (*90*) |
| $MnO_x$-$SnO_2$ | co-precipitation | 200 mg catalyst, 400 ppm HCHO, 10% $O_2$, 30,000 ml/g·h [4]GHSV | [1]100% at 220°C | (*90*) |
| Graphene−$MnO_2$ hybrid | Graphene treatment with $KMnO_4$ (redox) | 100 mg catalyst, 100 ppm HCHO, purified air, 30,000 mL/g·h [4]GHSV | [1]100% at 65°C | (*87*) |

[1] Conversion = $[CO_2]_{out}$ / $[HCHO]_{in}$
[2] Removal = ($[HCHO]_{in}$ - $[HCHO]_{out)}$ / $[HCHO]_{in}$
[3] RH - relative humidity
[4]GHSV- Gas hourly space velocity ($h^{-1}$ or ml/g.h)

Table 4

| Catalyst | Preparation method | Reaction conditions | HCHO removal | Reference |
|---|---|---|---|---|
| δ-$MnO_2$/PET 2 | Redox-precipitation | 500 mg catalyst, 0.6 mg/$m^3$ HCHO, purified air, 50% RH, 17,000/h [2]GHSV | 94% at 25°C | (*18*) |
| 8.86 wt% $MnO_2$/cellulose fiber 2 | $KMnO_4$ impregnation of cellulose fiber followed by oleic acid treatment | 5 mg catalyst, 100 ppm HCHO HCHO, 20 vol % $O_2$, 50 000/h [2]GHSV | 99.1% at 140°C | (*82*) |
| Birnessite/AC 2 | $KMnO_4$ reduction of | 200 mg catalyst, 400 ppm HCHO, synthetic air | 100% [1](25°C,7h) | (*98*) |
| δ-$MnO_2$/AC 2 | Redox co-precipitation | 100 mg catalyst, 150 ppm HCHO, pure air | 100% [1](25°C,9h) | (*71*) |

[1] Indicates the reaction temperature and time taken to reach such conversion in a static reactor.
[2]GHSV- Gas hourly space velocity ($h^{-1}$ or ml/g.h)

**Figure Captions**

Figure 1. (a) Effect of birnessite calcination temperature on HCHO oxidation activity at room temperature. (b) HCHO conversion and $CO_2$ generation (*73*). “Reproduced with permission from Wang, J.; Zhang, P.; Li, J.; Jiang, C.; Yunus, R.; Kim, J. Room-Temperature Oxidation of Formaldehyde by Layered Manganese Oxide: Effect of Water. Environ. Sci. Technol. 2015, 49 (20), 12372-12379. Copyright (2015) American Chemical Society”.

Figure 2. Effect of HCHO concentration on $Pt/MnO_x$-$CeO_2$ activity at room temperature. Reprinted (*48*). (Reproduced with permission from Tang, X.; Chen, J.; Huang, X.; Xu, Y.; Shen, W. Pt/MnOx–CeO2 catalysts for the complete oxidation of formaldehyde at ambient temperature. Appl. Catal., B 2008, 81 (1), 115-121. Copyright, 2008 Elsevier).

Figure 3. Concentration variation of HCHO and $CO_2$ formation in a static experiment: (a) over birnessite-$MnO_2$/AC (*98*) “Reproduced with permission from Li, J., Zhang, P., Wang, J. and Wang, M. Birnessite-Type Manganese Oxide on Granular Activated Carbon for Formaldehyde Removal at Room Temperature. J. Phys. Chem. C 2016, 120 (42), 24121-24129. Copyright (2016) American Chemical Society” and (b) over δ-$MnO_2$/AC (*71*). (Reproduced from Dai, Z.; Yu, X.; Huang, C.; Li, M.; Su, J.; Guo, Y.; Xu, H.; Ke, Q. Nanocrystalline $MnO_2$ on an activated carbon fiber for catalytic formaldehyde removal. RSC Adv. 2016, 6 (99), 97022-97029, with permission from The Royal Society of Chemistry).

Figure 4. Effect of reaction condition on the evolution of morphology and structure manganese based catalysts (*77*). (Reproduced with permission from Zhou, L.; Zhang, J.; He, J.; Hu, Y.; Tian, H. Control over the morphology and structure of manganese oxide by tuning reaction conditions

and catalytic performance for formaldehyde oxidation. Mater. Res. Bull. 2011, 46 (10), 1714-1722. Copyright, 2011 Elsevier).

Figure 5. Effect of tunnel structure on the complete oxidation of HCHO (*55*). (Reproduced with permission from Chen, T.; Dou, H.; Li, X.; Tang, X.; Li, J.; Hao, J. Tunnel structure effect of manganese oxides in complete oxidation of formaldehyde. Microporous Mesoporous Mater. 2009, 122 (1), 270-274. Copyright, 2009 Elsevier).

Figure 6. Formaldehyde conversion over transition metal catalysts as a function of reaction temperature.

Figure 7. Formaldehyde conversion over transition metal catalysts as a function of reaction time in a static system.

Figure 8. Synergistic Oxygen transfer mechanism in $MnO_x$-$CeO_2$ composites (*48*). (Reproduced with permission from Tang, X.; Chen, J.; Huang, X.; Xu, Y.; Shen, W. Pt/$MnO_x$–$CeO_2$ catalysts for the complete oxidation of formaldehyde at ambient temperature. Appl. Catal., B 2008, 81 (1), 115-121. Copyright, 2008 Elsevier).

Figure 9. Mechanism of HCHO oxidation on birnessite at RT (*73*). "Reproduced with permission from Wang, J.; Zhang, P.; Li, J.; Jiang, C.; Yunus, R.; Kim, J. Room-Temperature Oxidation of Formaldehyde by Layered Manganese Oxide: Effect of Water. Environ. Sci. Technol. 2015, 49 (20), 12372-12379. Copyright (2015) American Chemical Society".

Figure 10. Mechanism of HCHO oxidation over mesoporous $Co_3O_4$, Au/$Co_3O_4$, and Au/$Co_3O_4$-$CeO_2$ catalysts at RT (*51*). "Reproduced with permission from Ma, C.; Wang, D.; Xue, W.; Dou, B.; Wang, H.; Hao, Z. Investigation of Formaldehyde Oxidation over $Co_3O_4$−$CeO_2$ and Au/$Co_3O_4$−$CeO_2$ Catalysts at Room Temperature: Effective Removal and Determination of

Reaction Mechanism. Environ. Sci. Technol. 2011, 45 (8), 3628-3634. Copyright (2011) American Chemical Society".

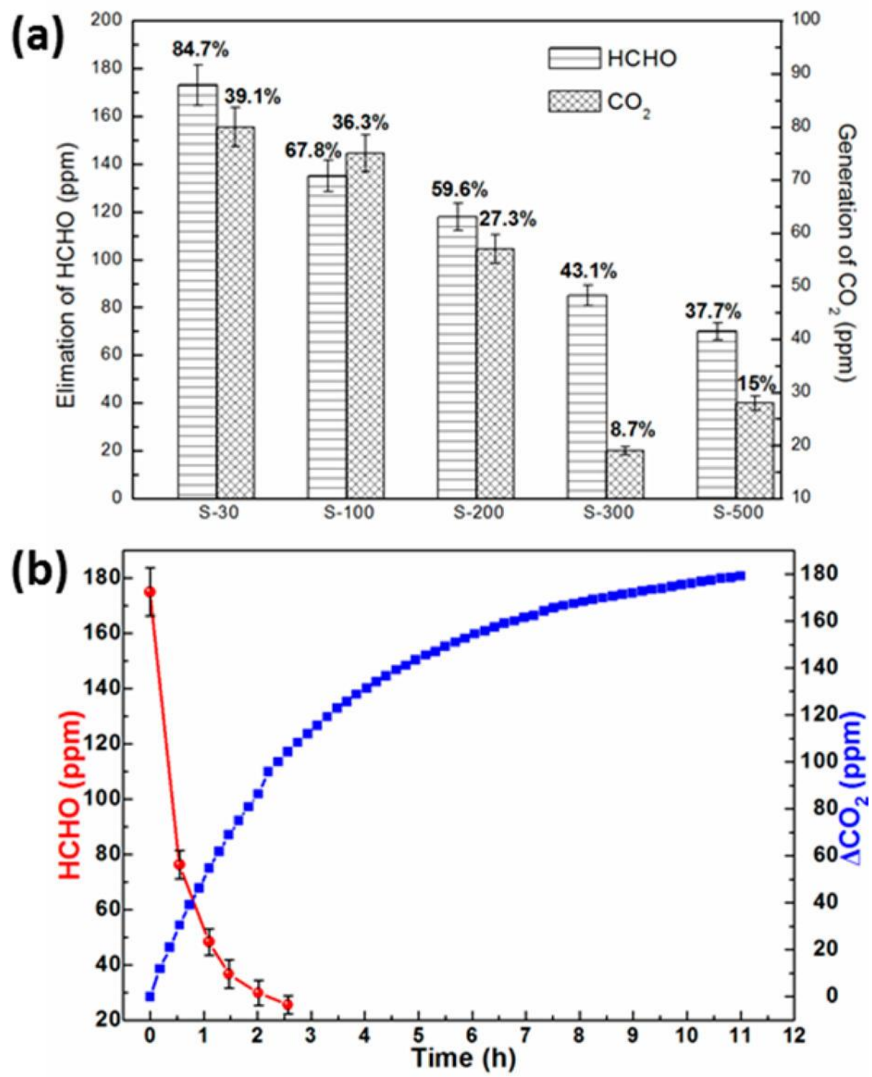

(a)
HCHO
CO2
84.7%
39.1%
67.8%
36.3%
59.6%
27.3%
43.1%
8.7%
37.7%
15%
Elimation of HCHO (ppm)
Generation of CO2 (ppm)
S-30
S-100
S-200
S-300
S-500
(b)
HCHO (ppm)
ΔCO2 (ppm)
Time (h)


Figure 1

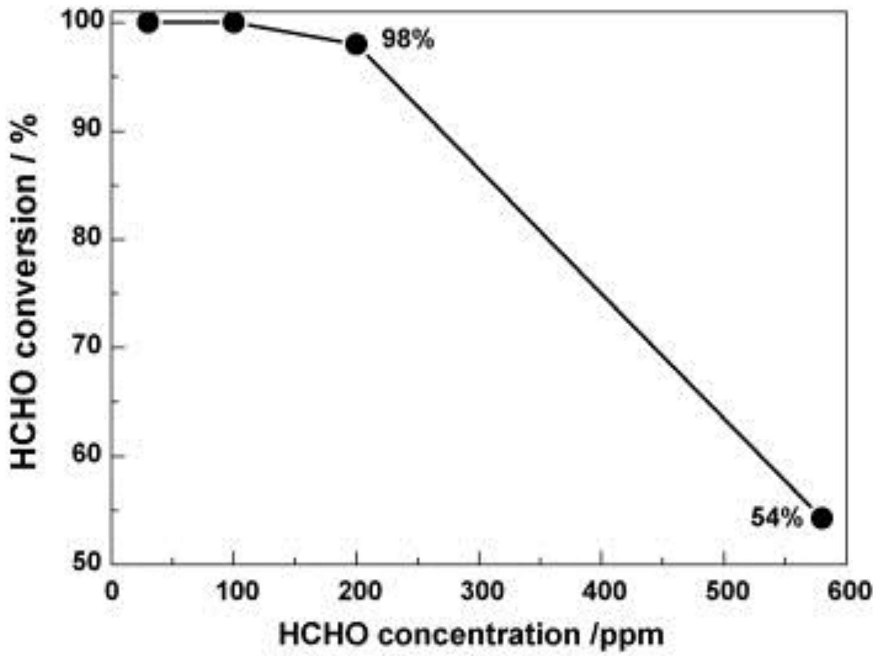
100
90
80
70
60
50
0
100
200
300
400
500
600
98%
54%
HCHO conversion / %
HCHO concentration /ppm

Figure 2

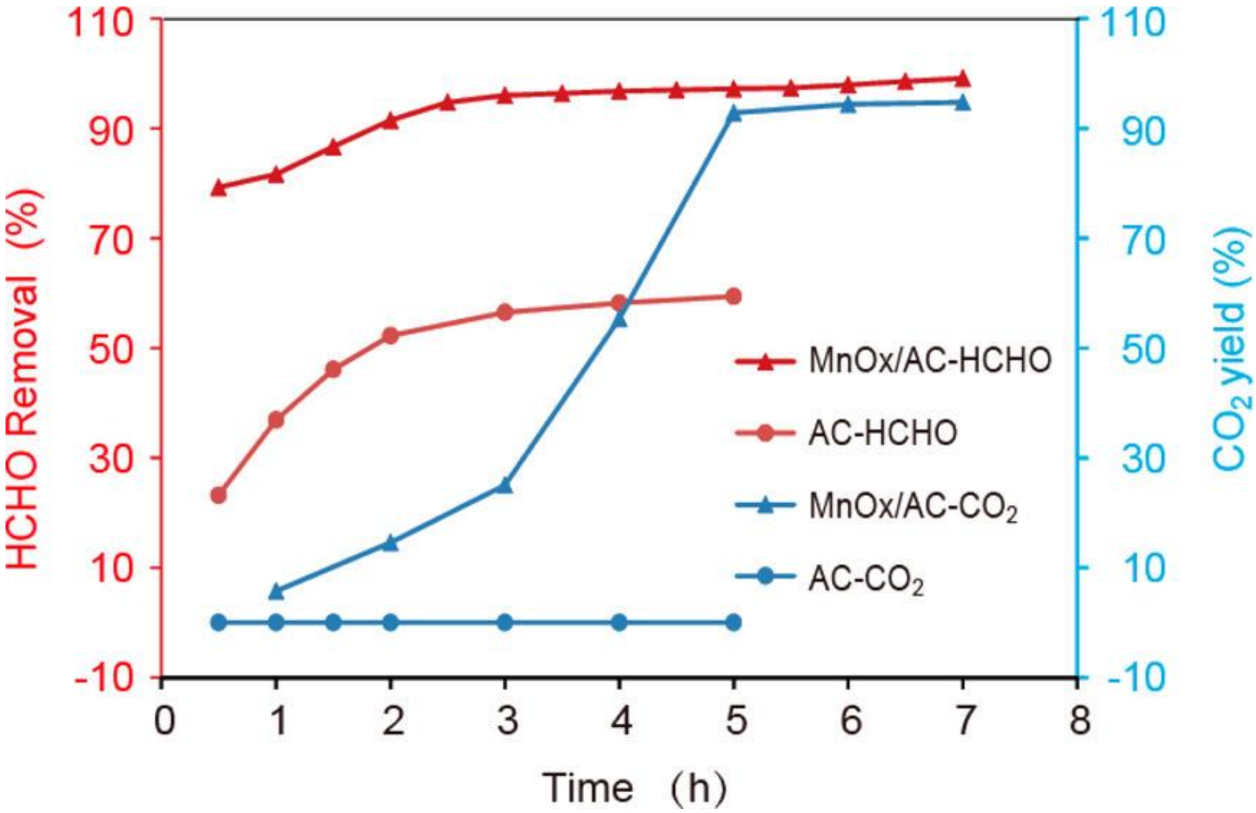
110
90
70
50
30
10
-10
HCHO Removal (%)
0
1
2
3
4
5
6
7
8
Time (h)
MnOx/AC-HCHO
AC-HCHO
MnOx/AC-CO2
AC-CO2
CO2 yield (%)

Figure 3(a)

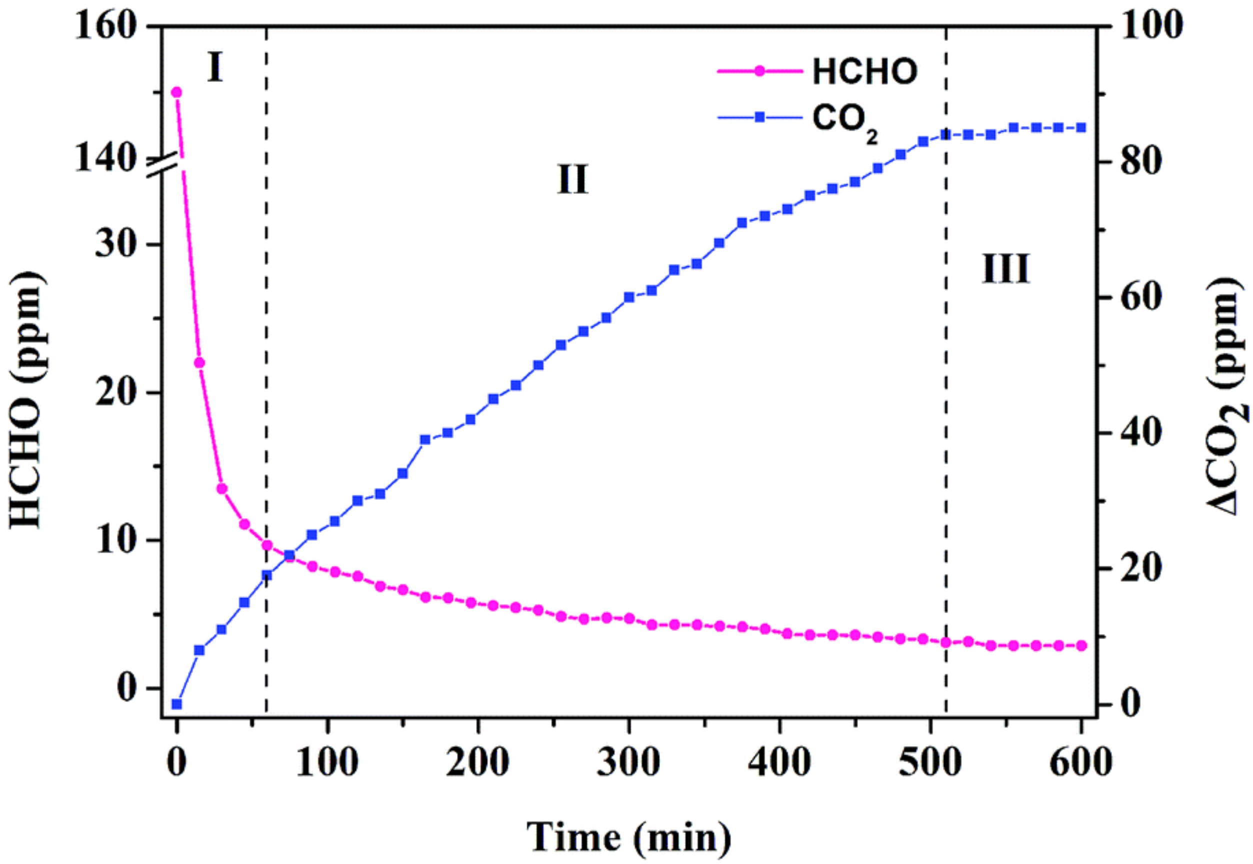
160
140
30
20
10
0
100
80
60
40
20
0
0
100
200
300
400
500
600
I
II
III
HCHO
CO2
HCHO (ppm)
ΔCO2 (ppm)
Time (min)

Figure 3(b)

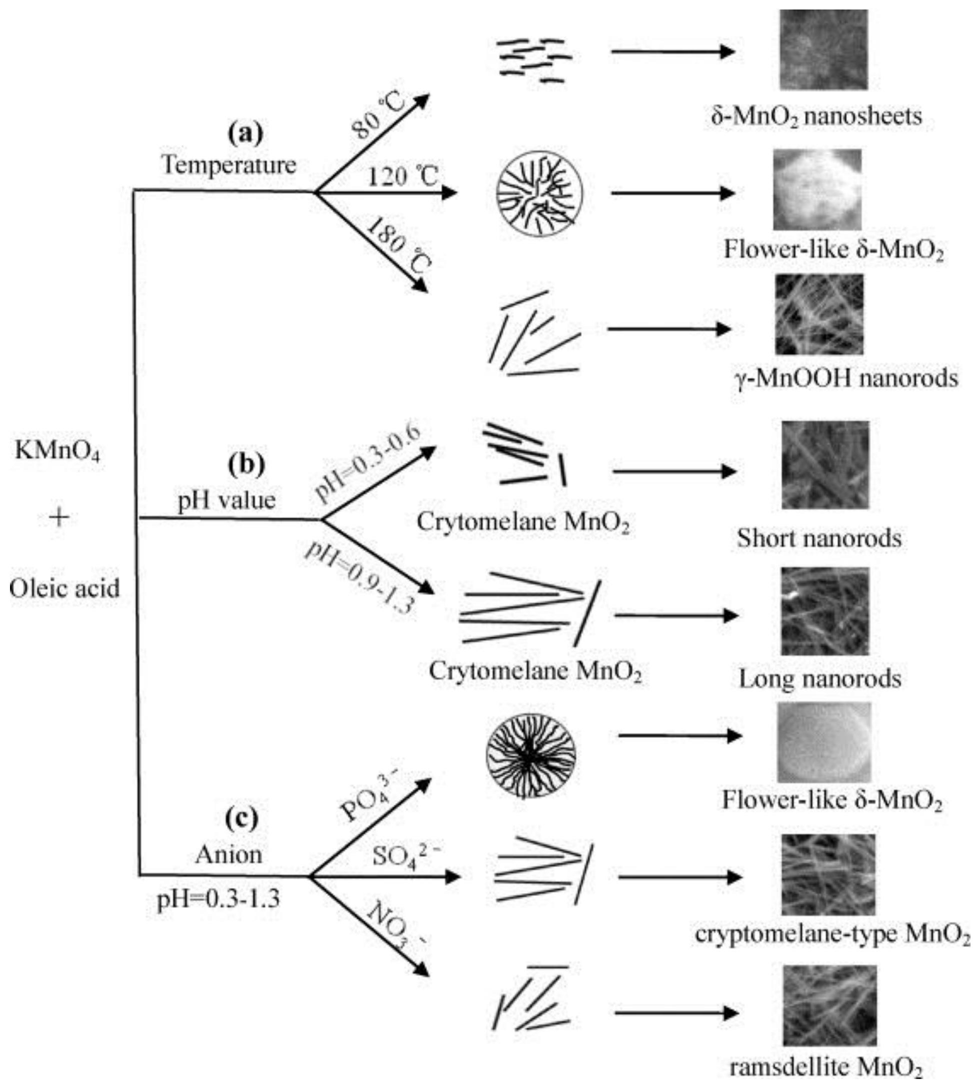

(a)
Temperature
80 ℃
120 ℃
180 ℃
δ-MnO2 nanosheets
Flower-like δ-MnO2
γ-MnOOH nanorods
KMnO4
+
Oleic acid
(b)
pH value
pH=0.3-0.6
pH=0.9-1.3
Crytomelane MnO2
Short nanorods
Crytomelane MnO2
Long nanorods
(c)
Anion
pH=0.3-1.3
PO4 3−
SO4 2−
NO3 −
Flower-like δ-MnO2
cryptomelane-type MnO2
ramsdellite MnO2


Figure 4

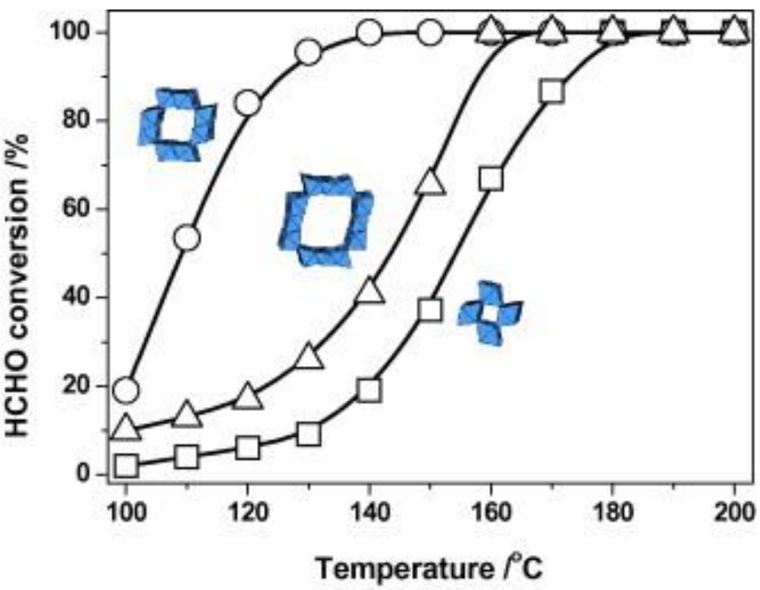
HCHO conversion /%
Temperature /°C
0
20
40
60
80
100
100
120
140
160
180
200

Figure 5

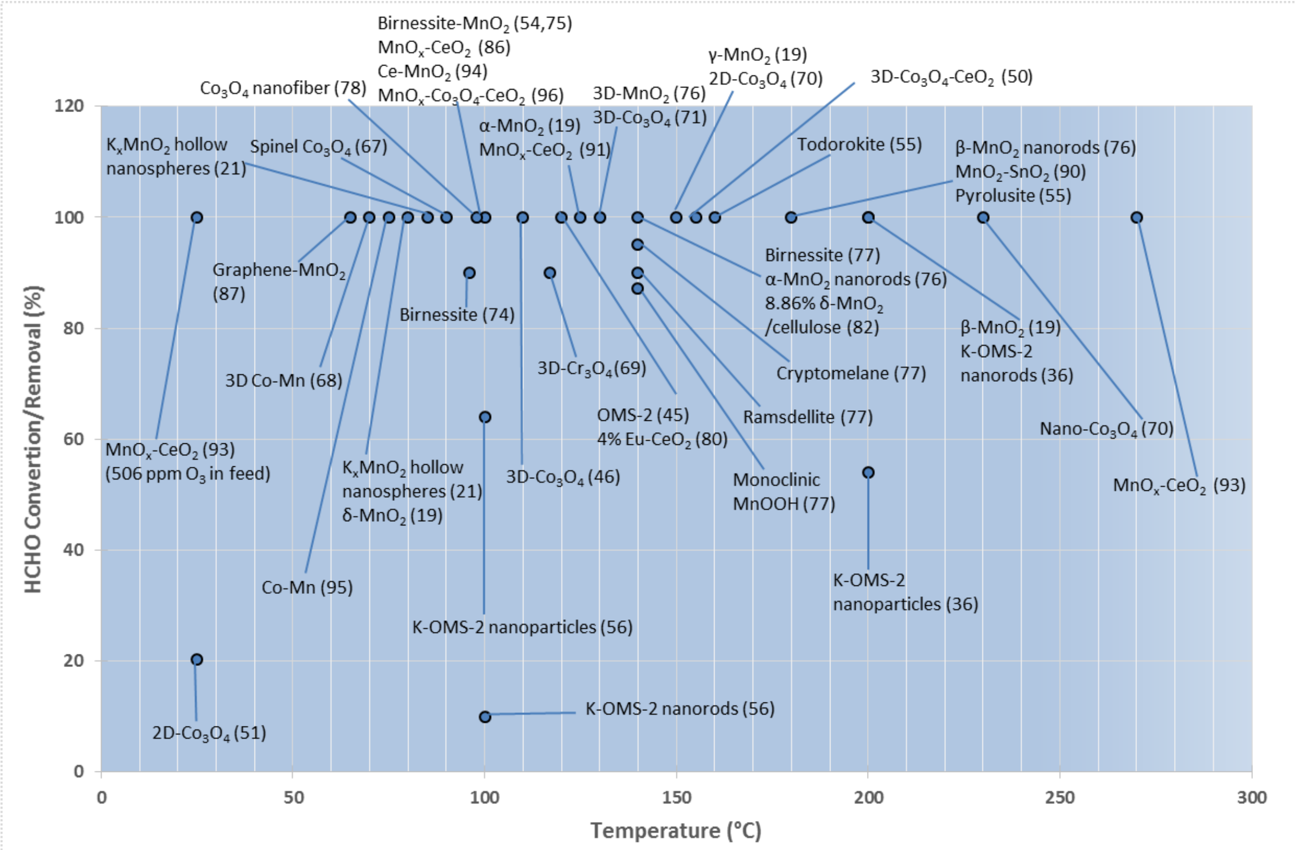

Birnessite-MnO2 (54,75)
MnOx-CeO2 (86)
Ce-MnO2 (94)
MnOx-Co3O4-CeO2 (96)
Co3O4 nanofiber (78)
γ-MnO2 (19)
2D-Co3O4 (70)
3D-Co3O4-CeO2 (50)
3D-MnO2 (76)
3D-Co3O4 (71)
α-MnO2 (19)
MnOx-CeO2 (91)
KxMnO2 hollow nanospheres (21)
Spinel Co3O4 (67)
Todorokite (55)
β-MnO2 nanorods (76)
MnO2-SnO2 (90)
Pyrolusite (55)
Graphene-MnO2 (87)
Birnessite (74)
Birnessite (77)
α-MnO2 nanorods (76)
8.86% δ-MnO2 /cellulose (82)
β-MnO2 (19)
K-OMS-2 nanorods (36)
3D Co-Mn (68)
3D-Cr3O4 (69)
Cryptomelane (77)
OMS-2 (45)
4% Eu-CeO2 (80)
Ramsdellite (77)
Nano-Co3O4 (70)
MnOx-CeO2 (93)
(506 ppm O3 in feed)
KxMnO2 hollow nanospheres (21)
δ-MnO2 (19)
3D-Co3O4 (46)
Monoclinic MnOOH (77)
MnOx-CeO2 (93)
Co-Mn (95)
K-OMS-2 nanoparticles (36)
K-OMS-2 nanoparticles (56)
K-OMS-2 nanorods (56)
2D-Co3O4 (51)
HCHO Convertion/Removal (%)
Temperature (°C)
0
20
40
60
80
100
120
0
50
100
150
200
250
300


Figure 6

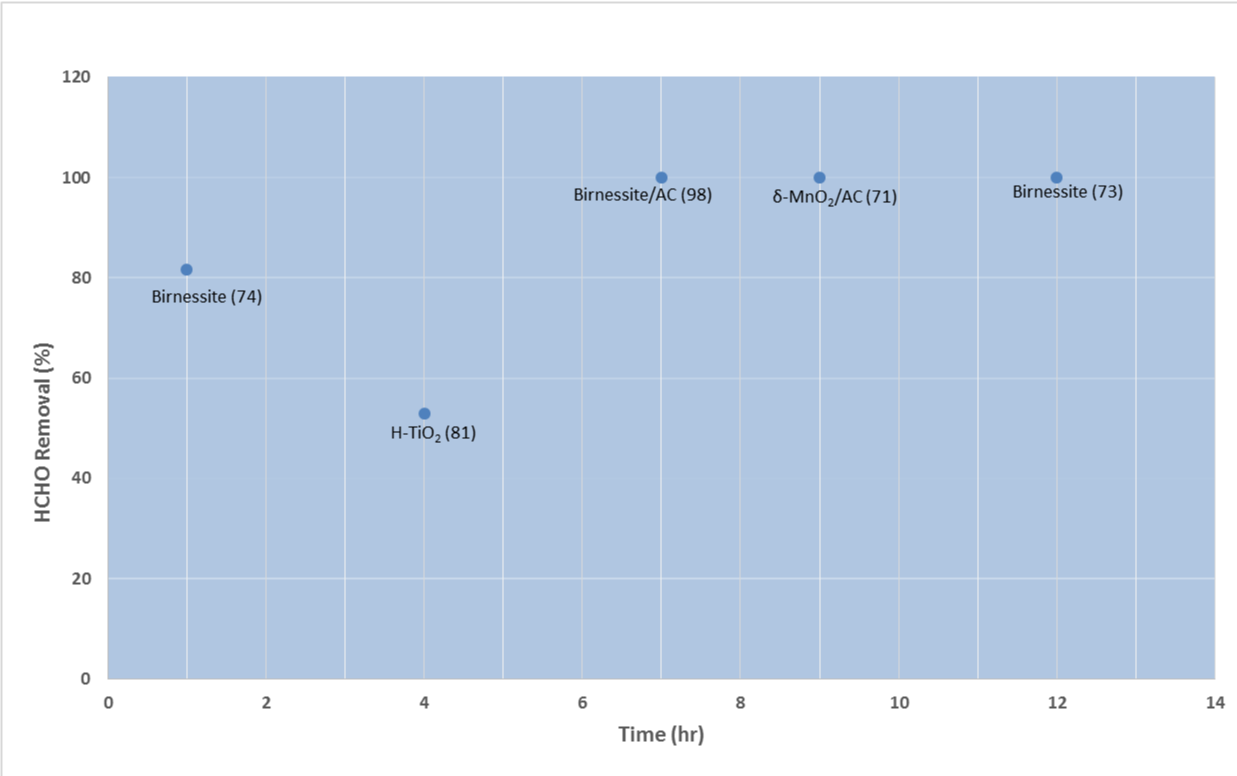
HCHO Removal (%)
Time (hr)
120
100
80
60
40
20
0
0
2
4
6
8
10
12
14
Birnessite (74)
H-TiO2 (81)
Birnessite/AC (98)
δ-MnO2/AC (71)
Birnessite (73)

Figure 7

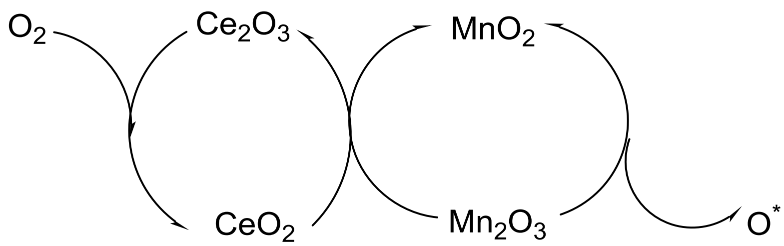


Figure 8

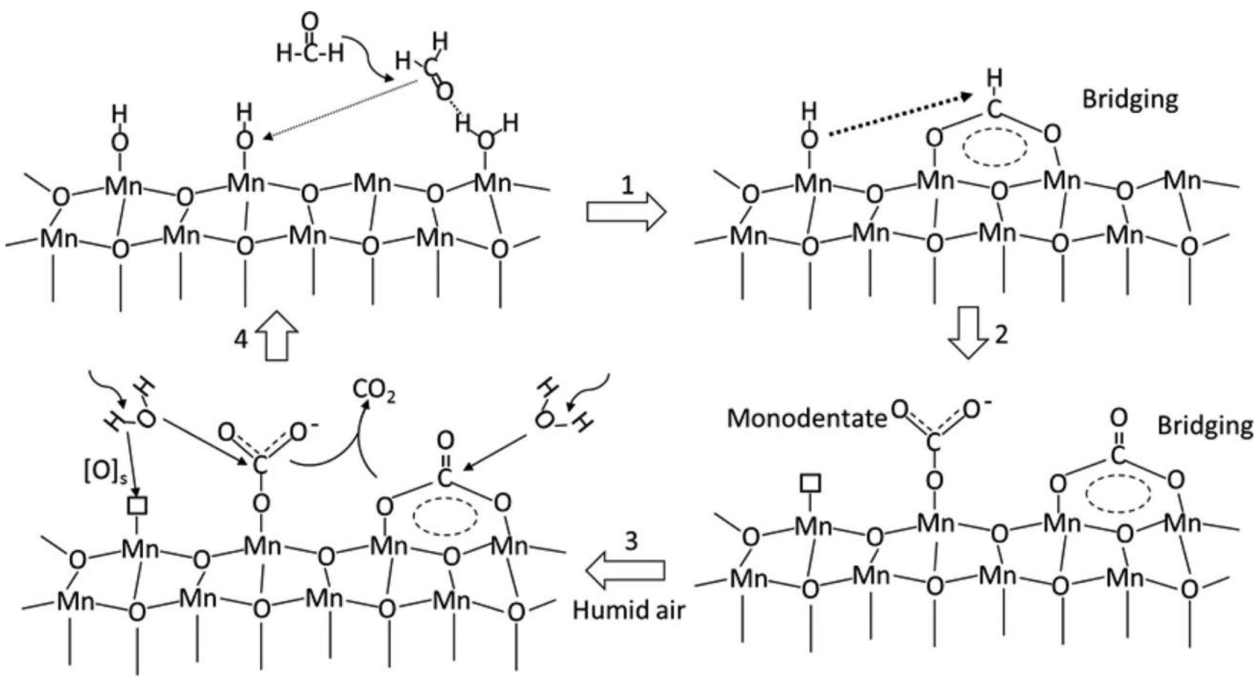


Figure 9

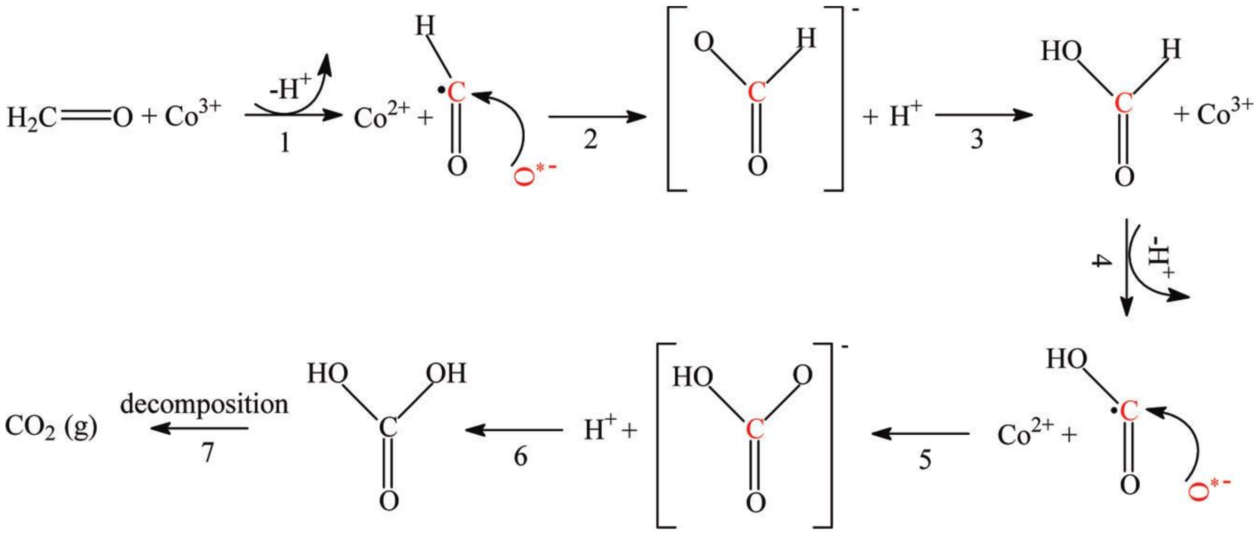

H₂C═O + Co3+
-H+
1
Co2+ +
H
C
O
O*-
2
O
H
C
O
+ H+
3
HO
H
C
O
+ Co3+
4
-H+
HO
C
O
Co2+ +
O*-
5
HO
O
C
O
H+ +
6
HO
OH
C
O
decomposition
7
CO2 (g)


Figure 10